



## Design and Analysis of a Compact Four-Port MIMO Antenna with Enhanced Isolation for UWB Applications

V N Koteswara Rao Devana<sup>1</sup>      Vanka Saritha<sup>2</sup>      N. R. Dhineshabu<sup>3</sup>  
 G. S. K. Gayatri Devi<sup>4</sup>      Nageswara Rao Lavuri<sup>5</sup>      Seepana Praveenkumar<sup>6</sup>  
 Hala K. Abduljaleel<sup>7</sup>      Ahmed Jamal Abdullah Al-Gburi<sup>8\*</sup>

<sup>1</sup>Electronics and Communication Engineering Department, Aditya University, Surampalem, A.P, India

<sup>2</sup>Department of Electronics and Communication Engineering,  
 Velagapudi Ramakrishna Siddhartha School of Engineering,

Siddhartha Academy of Higher Education (an institution deemed to be University), Vijayawada, AP, India

<sup>3</sup>Electronics and Communication Engineering Department,  
 T. John Institute of Technology, Bangalore, Karnataka, India

<sup>4</sup>Electronics and Communication Engineering Department,  
 Malla Reddy Engineering College, Hyderabad, Telangana, India

<sup>5</sup>Electronics and Communication Engineering Department,  
 CVR College of Engineering, Hyderabad, Telangana, India

<sup>6</sup>Department of Nuclear and Renewable Energy, Ural Federal University, Russia

<sup>7</sup>College of Engineering, Al-Iraqia University, Saba'a Abkar Complex, Baghdad, Iraq

<sup>8</sup>Centre for Telecommunication Research & Innovation (CeTRI), Fakulti Teknologi dan Kejuruteraan Elektronik dan Komputer (FTKEK), Universiti Teknikal Malaysia Melaka (UTeM), Malacca, Malaysia

\* Corresponding author's Email: [ahmedjamal@ieee.org](mailto:ahmedjamal@ieee.org)

---

**Abstract:** A compact four-port self-isolated multiple-input multiple-output (MIMO) antenna with enhanced isolation for ultrawideband (UWB) and X-band applications is presented. The proposed antenna is printed on an FR-4 substrate with a size of  $35 \times 35 \text{ mm}^2$  and features embedded elliptical, circular, and rectangular structures as the radiating patch, along with a semi-elliptical defected ground structure (SE-DGS). The antenna operates over a frequency range of 3.91 GHz to beyond 15 GHz, achieving a peak gain of 5.41 dBi, a peak radiation efficiency of 92.84%, and an isolation of more than 30 dB across the operating band for UWB and X-band applications. The diversity characteristics include an envelope correlation coefficient (ECC) of less than 0.001, a diversity gain (DG) exceeding 9.99 dB, and a mean effective gain (MEG) lower than -3.01 dB, all achieved without the need for additional coupling elements among the antenna elements. The simulated results of the proposed antenna show a strong correlation with the measured results, making it a promising candidate for UWB-MIMO applications.

**Keywords:** Defected ground structure (DGS), Diversity, Multiple-input-multiple-output (MIMO), Self-isolation, Ultrawideband (UWB).

---

### 1. Introduction

In these days, interference-free data throughput is highly sought for. In order to increase the capacity of a radio connection, MIMO technology makes use of several transmit and receive elements to accomplish multipath propagation [1, 2]. By using all the features

of wireless communication systems, a MIMO system improves the capacity of communication channels, the dependability of networks, and the speed of data transfer in various types of wireless networks. It is essential to put the antennas in close proximity to one another in order to achieve the aforementioned properties. Wireless communication systems have recently begun to focus on UWB technology because

of its cheap manufacturing cost and high data speeds [3, 4]. The primary issues with UWB technology that led to multipath fading are the reflection and diffraction of electromagnetic waves in dense media. In order to keep up with the ever-increasing demand for wireless communication, future communication networks will relentlessly pursue faster data rates. High data rates, even 1Gb/s, need the deployment of more sophisticated technologies. Since both UWB and MIMO technologies have the potential to increase communication speeds, combining them might be the best option [5]. Modern intelligent wireless applications rely on sophisticated antenna designs for UWB and MIMO communication systems. Its main contributions to high-performance wireless communication technologies are better isolation, a small size, and diversity features. These are necessary for making smart engineering solutions for the Internet of Things (IoT) and high-data-rate communication. In addition, the smart design of a small four-port MIMO antenna that is more efficient and has better isolation helps smart systems work with cutting-edge communication technologies. The mutual coupling increases as the distance between the antenna components decreases. For a MIMO system to function efficiently, the selected distance must be between  $\lambda/4$  and  $\lambda/2$  in order to achieve a coupling of  $< 15$  dB. The more the distance between antenna units, the bigger the MIMO system becomes. Therefore, it is important to consider the trade-offs between limiting mutual coupling and maximizing the overall size of MIMO systems while constructing MIMO antennas [6, 7]. In literature, there are so many MIMO antennas with four ports for wide band and UWB applications is reported [8-17]. Table 1 compares the suggested MIMO element performance to that of previously disclosed antennas.

From Table 1, it is noticed that the suggested four element antenna size is compact ( $1225 \text{ mm}^2$ ) compared to [8] of ( $13,310 \text{ mm}^2$ ), [9] of ( $8,649 \text{ mm}^2$ ), [10] of ( $8,100 \text{ mm}^2$ ), [11] of ( $3,364 \text{ mm}^2$ ), [12] of ( $2,296 \text{ mm}^2$ ), [13] of ( $1,764 \text{ mm}^2$ ), [14] of ( $1,600 \text{ mm}^2$ ), [15] of ( $1352 \text{ mm}^2$ ), [16] of ( $1,296 \text{ mm}^2$ ), and [17] of ( $1,600 \text{ mm}^2$ ). The recommended antenna operates at a broader bandwidth of (3.91 to  $>15$  GHz) compared to 2-6 GHz [8], 3-13 GHz [9], 3.56 and 5.28 GHz [10], 2.8-12.1 GHz [11], 3.4-11.8 GHz [12], 3.09-12 GHz [13], 3.2-13.4 GHz [14], 3-12.3 GHz [15], 2-11.08 GHz [16] and 2.8-11.4 GHz [17]. A better isolation of  $>30$  dB is provided by the suggested antenna over  $>16.36$  dB [8],  $>20$  dB [9],  $>20$  dB [10],  $>20$  dB [11],  $>18$  dB [12],  $>14$  dB [13],  $>22$  dB [14],  $>15$  dB [15],  $>18$  dB [16] and  $>26$  dB [17]. The peak gain of proposed antenna is 5.41 dBi, which is better to 5.4 dBi [9], 4.2 dBi [10], 4.1 dBi

[12], 5.1 dBi [13], and 5.2 dBi [16] and also the peak efficiency of 92.84% is satisfactory over 88.34% [10], 91% [12], 82% [13], and 90% [16, 17] with most of the comparison works not reported. The MIMO diversity characteristics of proposed antenna such as ECC  $<0.0001$  is minimum over 0.04 [8], 0.003 [9],  $<0.04$  [10], 0.03 [11], 0.002 [12],  $<0.02$  [13], 0.05 [14],  $<0.43$  [15],  $<0.4$  [16], and  $<0.001$  [17] and DG is maximum at 9.99 dB compared to 9.85 dB [10], 9.98 dB [15], and 9.9 dB [17]. Various reported works have utilized different coupling structures to enhance isolation, including parasitic elements such as Z-shaped structures [8], cross-hook-shaped strips [11], cruciform rotating strips [13], plus-sign-shaped conducting strips [14], and fan-shaped parasitics [16]. Additionally, stubs like ground plane with stub [9], I-shaped stubs [15], and plus-form stubs [17], as well as Defected Ground Structures (DGS) [12], have been employed for isolation improvement. The antenna presented in [10] adopts an orthogonal arrangement of elements without additional coupling structures, similar to the proposed work; however, its larger size remains a key limitation compared to the compact design of the proposed antenna. In all the above reported MIMO elements [8-17], the antennas are proposed for wide band and UWB applications with different patch and ground structures to achieve the required band of operation and to reduce the coupling. The proposed antenna's semi-elliptical defected ground structure (SE-DGS) and robust FR-4 substrate help maintain stable performance under varying environmental conditions such as temperature and humidity. While scalability is feasible for higher frequencies, future improvements will focus on further enhancing the antenna's environmental resilience and adaptability for outdoor applications.

The merits of the proposed work are summarized as follows:

- (i) Compact size ( $35 \times 35 \text{ mm}^2$ )
- (ii) A compact and novel structure etched on a low-cost FR-4 substrate operating over 3.91 to more than 15 GHz.
- (iii) The gain is 5.41 dBi (peak) and efficiency of 92.84% (peak) over working band.
- (iv) The antenna provides isolation of more than 30 dB without use of coupling element.
- (v) The diversity characteristics such as ECC of  $<0.001$ , and DG of 9.9999 over 3.91 to more than 15 GHz makes it suitable for extended UWB applications.

Table 1. Performance comparison.

Ref.	Size (mm <sup>2</sup> )	Area (mm <sup>2</sup> )	Number of Ports	B.W (GHz)	S <sub>21</sub> (dB)	Peak Gain (dBi)	R.E (%)	ECC	DG (dB)
[8]	121×110	13,310	4	2-6	>16.36	5.97	NR	<0.04	<10
[9]	93×93	8,649	4	3-13	>20	5.4	NR	<0.003	>9.99
[10]	90×90	8100	4	3.56-5.28	>22	4.2	88.34	<0.04	9.85
[11]	58×58	3364	4	2.8-12.1	>15	6.57	97	<0.03	10
[12]	56×41	2296	4	3.4-11.8	>20	4.1	91	<0.002	9.99
[13]	42×42	1764	4	3.09-12	>16.4	5.1	82	<0.02	9.991
[14]	40×40	1600	4	3.2-13.4	>20	NR	NR	<0.05	9.99
[15]	26×52	1352	4	3-12.3	>15	NR	NR	<0.43	9.98
[16]	36×36	1296	4	2-11.08	>15	5.2	90	<0.4	NR
[17]	40×40	1600	4	2.8-11.4	>26	6	90	<0.001	9.9
<b>Pro.</b>	<b>35×35</b>	<b>1225</b>	<b>4</b>	<b>3.91-&gt;15</b>	<b>&gt;30</b>	<b>5.41</b>	<b>92.84</b>	<b>&lt;0.0001</b>	<b>&gt;9.99</b>

Pro.- Proposed, B.W- Bandwidth, R.E- Radiation Efficiency, NR- Not Reported.

The present work is focused to design and development a four-port self-isolated MIMO antenna for extended UWB applications with improved isolation without coupling element. The suggested design is a combination of ellipse and circular patches with a triangular feed, and a semi-elliptical DGS with self-isolation characteristics. The work is organized into following sections: section 2 describes the antenna design, section 3 includes the step-by-step implementation of proposed single element patch and ground structures with parametric analysis, section 4 elaborates the simulated and measured results along with diversity characteristics and finally conclusions are discussed in section 5.

### 2. Antenna design

The four elements of the proposed MIMO are placed orthogonally to each other in reducing the mutual coupling and to achieve the desired diversity characteristics. The elements are printed on a low-cost 35×35 mm<sup>2</sup> size FR-4 substrate with the combination of elliptical, circular and rectangular patches along with semi-elliptical DGS as depicted in Fig. 1. The optimized dimensions of reported MIMO are (in mm): W=35, L=35, a=9, b=4.63, c=3, d=1, e=7, f=7.5. The proto type of the radiator is shown in Fig. 2.

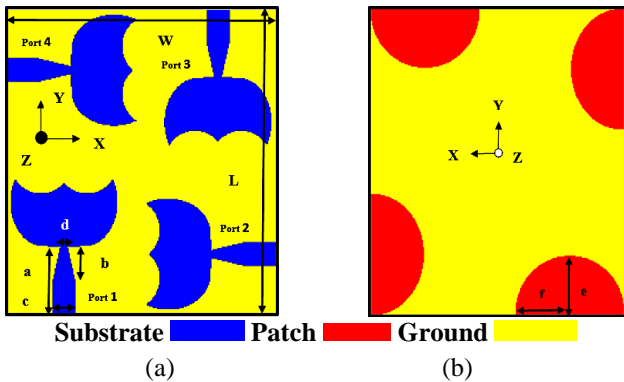


Figure. 1 Geometry of MIMO: (a) Top view and (b) Bottom view

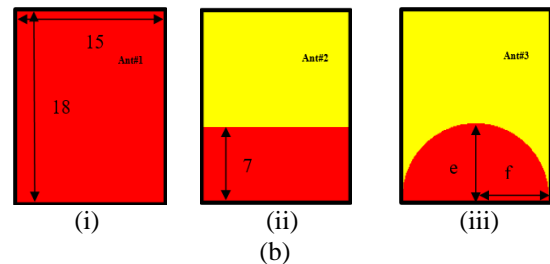
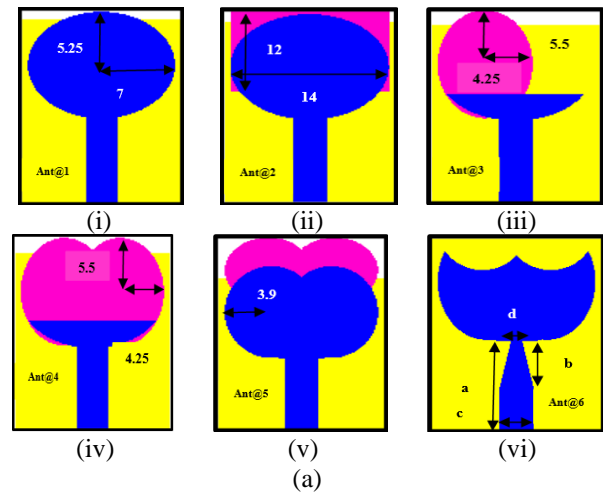


Figure 3. Implementation of: (a) Patch and (b) Ground structures

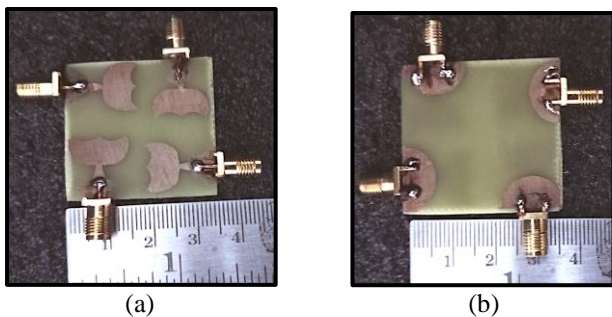


Figure. 2 Prototype: (a) Top view and (b) Bottom view

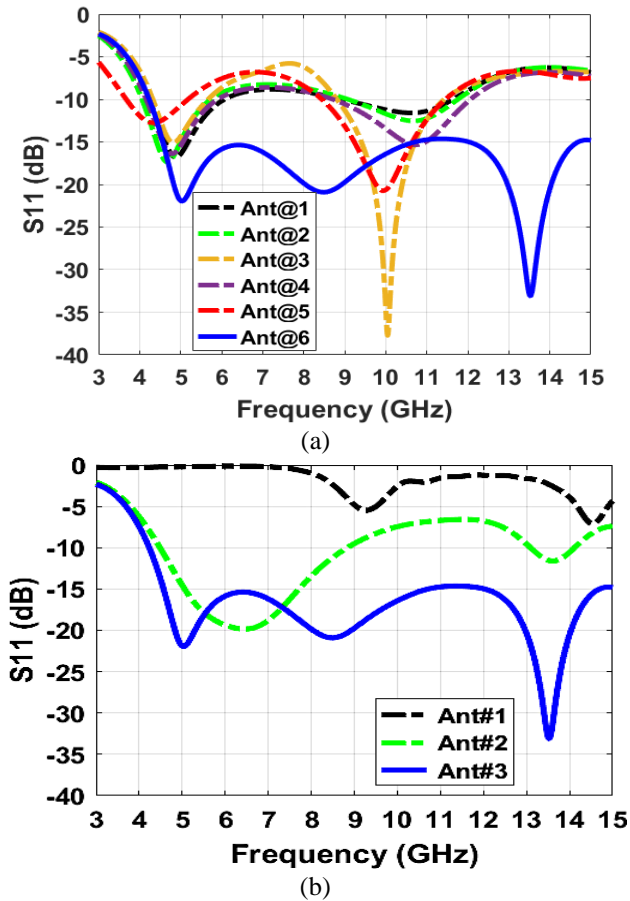


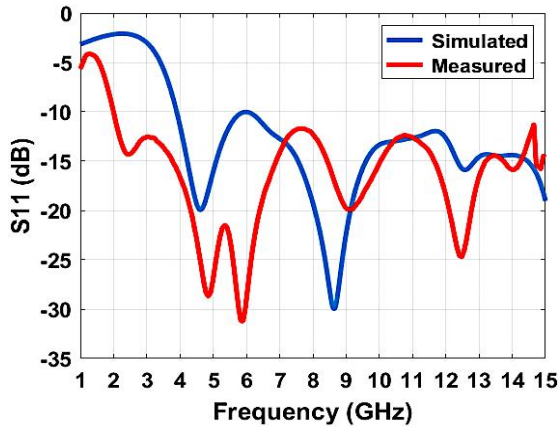
Figure. 4  $S_{11}$  parameters in different stages with: (a) patch and (b) ground structures.

### 3. Evolution of antenna

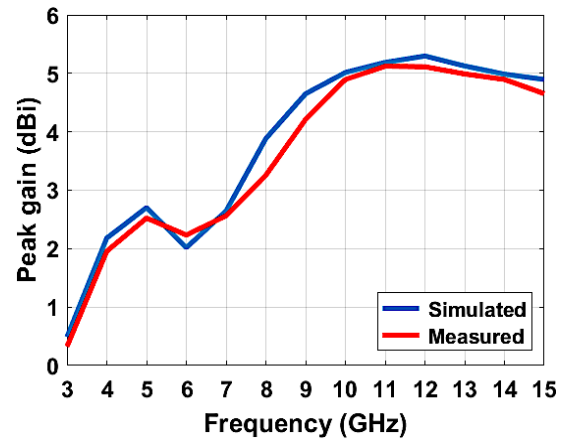
Fig. 3 depicts the evolution of proposed single element patch and ground structures in different stages. The basic element of intended radiator is designed with an ellipse having major radii of 7 mm and minor radii of 5.25 mm as depicted in Fig. 3 (a) (i). A purple-colored rectangular structure of  $14 \times 12$  mm<sup>2</sup> is etched as in Fig. 3 (a) (ii) and then two purple-colored ellipses of major and minor radii 5.5 mm and 4.25 mm are embedded to Ant@2 for obtaining the structures shown in Fig. 3 (a) (iii) and (iv). In the next stage, two purple-colored circles of radius 3.9 mm are added as in Fig. 3 (a) (v) and then subtracted as depicted Fig. 3 (a) (vi) along with a tapered feed [18] to obtain the desired UWB bandwidth. Circular and elliptical shapes can enhance the bandwidth due to their ability to support multiple modes of current distribution, providing wider operational bandwidth than standard rectangular patches [19-21]. The SE-DGS as depicted in Fig. 3 (b) (iii) is obtained from full ground structure of  $15 \times 18$  mm<sup>2</sup> as in Fig. 3 (b) (i) and then it is etched with a partial rectangular DGS of  $15 \times 7$  mm<sup>2</sup> as in Fig. 3 (b) (ii). The simulated  $S_{11}$  of the radiator in different stages of patch and ground implementation are depicted in Fig. 4 (a) and (b). The parametric analysis is carried out with patch, and ground structures is represented in Table 2.

Table 2. Parametric analysis with varying patch and ground.

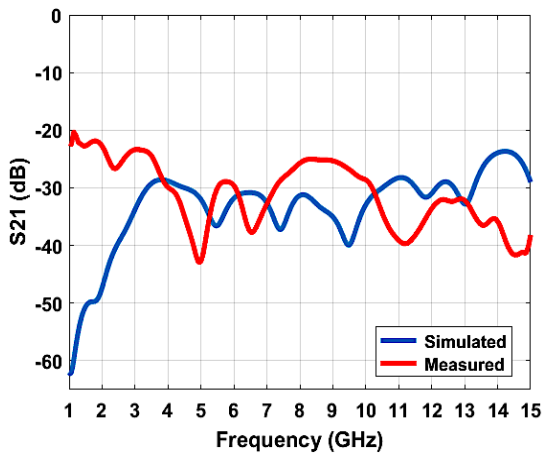
Varying Parameter	Structure	No. of resonances	Resonant frequencies (GHz)	Bandwidth (GHz)	Peak of $S_{11}$ (dB)
Patch		2	4.88, 10.62	4.25-6.07, 8.97-11.62	-16.8, -11.59
		2	4.68, 10.68	4.09-5.72, 9.10-11.77	-17.37, -12.53
		2	4.82, 10.04	4.3-5.67, 8.82-11.41	-15.09, -37.73
		2	4.78, 10.75	4.17-5.88, 8.73-12.09	-16.4, -15.33
		2	4.33, 9.93	3.67-5.2, 8.45-11.53	-12.75, -20.73
		3	5.03, 8.49, 13.53	4.25- >15	-21.94, -20.9, -33.1
Ground		-	-	-	-
		2	6.44, 13.6	4.49-8.82, 13.08-14.14	-19.83, -11.6
		3	5.03, 8.49, 13.53	4.25- >15	-21.94, -20.9, -33.1



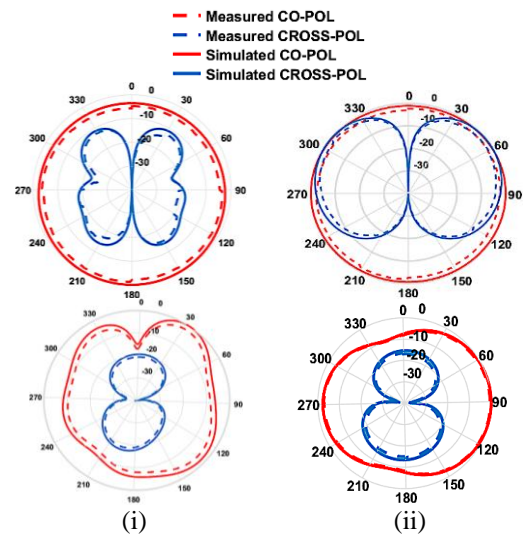
(a)



(e)



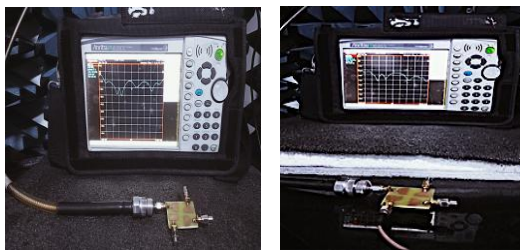
(b)



(i)

(ii)

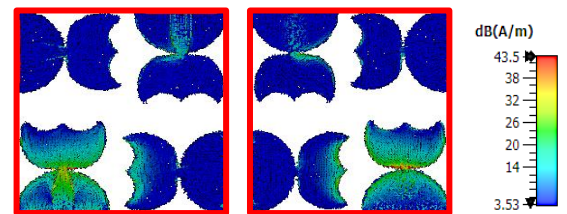
(f)



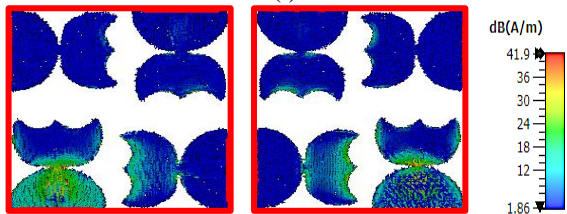
(i)

(ii)

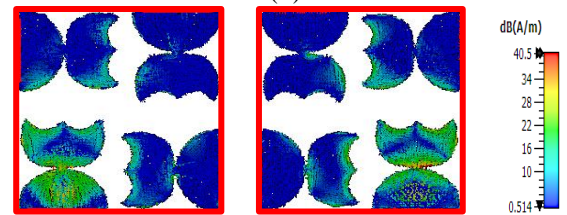
(c)



(i)

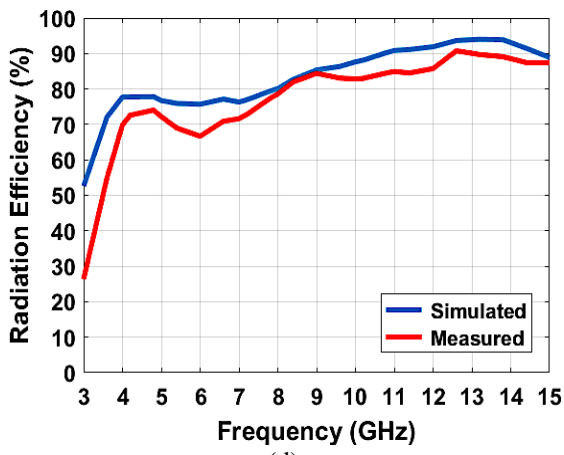


(ii)



(iii)

(g)



(d)

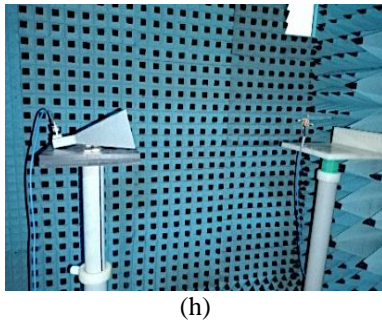


Figure. 5 Frequency domain characteristics: (a) Simulated and measured  $S_{11}$  Parameter, (b) Simulated and measured  $S_{21}$  Parameter, (c) Photograph of measured S- parameters: (i)  $S_{11}$ , and (ii)  $S_{21}$ , (d) Efficiency, (e) Gain, (f) Radiation patterns: (i) At 4.78 GHz, and (ii) At 8.68 GHz, (g) Surface current distribution: (i) Front and rear view at 4.78 GHz with port 1 excited, (ii) Front and rear view at 8.68 GHz with port 1 excited, and (iii) Front and rear view at 12.84 GHz with port 1 excited, and (h) Proposed antenna in anechoic chamber

## 4. Results and discussions

### 4.1 Radiation characteristics

Fig. 5 (a) and (b) depicts comparison of simulated and observed S-parameter values. From Fig. 5 (a), the radiator functions over 3.91 to >15 GHz (simulated) with three resonances at (4.78 GHz, 8.68 GHz, 12.84 GHz) having peak  $S_{11}$  of (-19.92 dB, -29.98 dB, -16.23 dB), respectively and operates over 2 to >15 GHz (measured) with five resonances at (2.34 GHz, 4.84 GHz, 5.88 GHz, 9.07 GHz, 12.48 GHz) with peak  $S_{11}$  of (-14.23 dB, -27.82 dB, -31.85 dB, -20 dB, -24.88 dB), covering UWB band with good match of impedance properties. From Fig. 5 (b), an improved isolation of  $S_{21}>30$  dB (simulated) and  $S_{21}>25$  dB (measured) over most of the working band.

The simulated and observed results are almost identical; nevertheless, there is a little discrepancy due to conductive, losses of SMA connector, dielectric, and also as manufacturing tolerances. The main reasons for the small differences between the simulations and measured parameters include conductive losses in the FR-4 material, manufacturing imperfections in the fabrication process, and testing setup-related connection losses. Resonance frequency shifts and decreased efficiency at higher frequencies have been caused by soldering discrepancies and substrate inhomogeneity. The photographs of measurement of  $S_{11}$  and  $S_{21}$  parameters are depicted in Fig. 5 (c). The proposed design achieves a peak radiation efficiency of 92.84% (simulated) at 13.82 GHz and 90.62% (measured) at 12.64 GHz with an average efficiency over the operating band are to be 85.38% (simulated) and

82.13% (measured) as depicted in Fig. 5 (d). The peak gain is 5.41 dBi (simulated) at 12 GHz and 5.18 dBi (measured) at 11.05 GHz with average gain of 4.35 dBi (simulated) and 4.12 dBi (measured) over the working band as in Fig. 5 (e). The E and H-plane simulated and measured patterns at resonant frequencies of 4.78, and 8.68 GHz are in Fig. 5 (f), from which it is understood that H-fields are omni and E-fields are bi-directional patterns [22]. The surface currents at 4.78, 8.68 and 12.84 GHz for the recommended radiator when port 1 is excited in front and rear view are illuminated in Fig. 5 (g). At three resonant frequencies, the radiating elements concentrate the majority of the surface current, while the ground plane distributes a smaller amount. This demonstrates that the MIMO antenna is an efficient radiator [23]. Fig. 5 (h) displays the photograph of the element in an anechoic chamber to test its radiation properties.

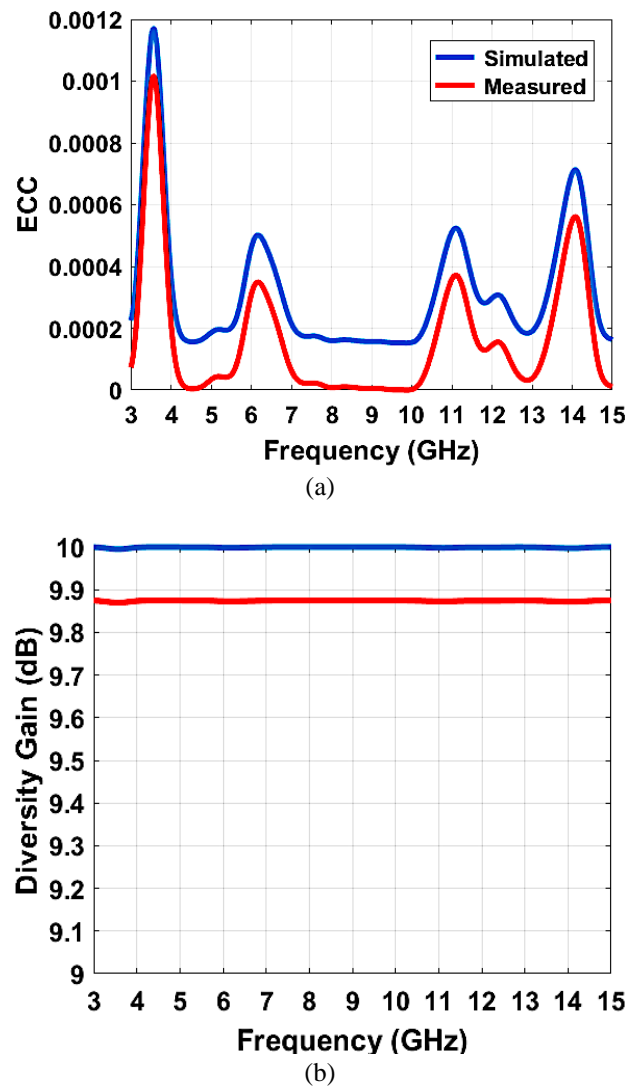


Figure. 6 MIMO Diversity characteristics: (a) ECC and (b) Diversity Gain

## 4.2 MIMO diversity characteristics

The ECC [24], which defines the correlation between the channels, is symbolized by Eqs. (1) and (2) for a four-element system. ECC, where 0 indicates no correlation and 1 indicates a high level of correlation among both signals, is represented by equations (1) and (2) for a two-element system. ECC values below 0.5 are considered acceptable for use in practice. The suggested four-element MIMO antenna's simulated and calibrated ECC are in Fig. 6 (a). The lowest ECC value is 0.00016 in the simulation and 0.000012 in the measurement, indicating that the suggested structure provides <0.001 over the whole spectrum. The compact design prioritizes space-saving and integration into portable devices, which may slightly reduce diversity performance compared to larger antennas. However, the proposed antenna achieves a balanced trade-off with an ECC of <0.001 and DG >9.99 dB, which remains comparable to larger antennas [8-17] while maintaining superior isolation and wideband coverage.

$$ECC_{ij} = \frac{|S_{ii}S_{jj} - S_{ij}S_{ji}|^2}{(1 - |S_{ii}|^2 - |S_{ij}|^2)(1 - |S_{jj}|^2 - |S_{ji}|^2)} \quad (1)$$

$$DG = 10\sqrt{1 - ECC^2} \quad (2)$$

Where,  $S_{ii}$  and  $S_{jj}$  are the reflection coefficients of antennas  $i$  and  $j$  and  $S_{ij}$  and  $S_{ji}$  are the mutual coupling coefficients between antennas  $i$  and  $j$ .

One way to see how well different antenna diversity methods work is by looking at their DG [24]. Using Equation (3), we can assess how well the suggested MIMO antenna diversity system performs with orthogonal arrangements of antenna elements [25]. Fig. 6 (b) displays the plots of the measured and simulated DG. Over the working band, the peak DG of 9.9965 dB (simulation) and 9.8998 dB (measured) is achieved. Thus, the proposed antenna operating over UWB integrated with partial Ku band with a compact size is suitable contender for wireless UWB applications with improved isolation.

## 5. Conclusion

This work presents a compact and novel shaped four element MIMO radiator with self-isolation for extended UWB wireless applications. The patch structure consists of the embedded ellipses, circles, rectangle and a triangular feed structure etched on top of low-cost FR-4 substrate and a semi-elliptical DGS is printed on bottom of substrate. The recommended

element is suitable for UWB applications operating over 3.91 to more than 15 GHz with a gain of 5.41 dBi (peak), radiation efficiency of 92.84% (peak) along with diversity characteristics of  $ECC < 0.001$ , and  $DG \approx 9.99$  dB. The radiator simulation findings agree well with measured results, confirms that the reported radiator is good choice for portable UWB wireless applications. The design that was suggested works well in the ultra-wideband and X-band frequencies. However, it would be hard to make it work at higher frequencies, like mm wave bands, because of manufacturing tolerances and higher dielectric losses. To keep isolation while minimizing performance trade-offs at higher frequencies, the ground structure and parasitic components will need to be optimized even more for multi-band integration.

## Conflicts of Interest

The authors declare no conflict of interest.

## Author Contributions

V N Koteswara Rao Devana; software, V N Koteswara Rao Devana; validation, V N Koteswara Rao Devana, Vanka Saritha, and N. R. Dhineshabu; formal analysis, G. S. K. Gayatri Devi; investigation, Nageswara Rao Lavuri; resources, Seepana Praveenkumar; data curation, V N Koteswara Rao Devana and Ahmed Jamal Abdullah Al-Gburi; writing—original draft preparation, Hala K. Abduljaleel and Ahmed Jamal Abdullah Al-Gburi; writing—review and editing, V N Koteswara Rao Devana; visualization, V N Koteswara Rao Devana; supervision, Ahmed Jamal Abdullah Al-Gburi; project administration, Hala K. Abduljaleel and Ahmed Jamal Abdullah Al-Gburi; funding acquisition.

## Acknowledgments

The authors would like to thank Universiti Teknikal Malaysia Melaka (UTeM) and the Ministry of Higher Education (MOHE) of Malaysia for supporting this project.

## References

- [1] P. Kumar, A. K. Singh, R. Kumar, S. K. Mahto, P. Pal, R. Sinha, A. Choubey, and A. J. A. Al-Gburi, "Design and Analysis of Low Profile Stepped Feedline with Dual Circular Patch MIMO Antenna and Stub Loaded Partial Ground Plane for Wireless Applications", *Progress In Electromagnetics Research C*, Vol. 140, pp. 135-144, 2024.
- [2] P. Kumar, A. K. Singh, R. Kumar, R. Sinha, S. K. Mahto, A. Choubey, and A. J. A. Al-Gburi,

- "High Isolated Defected Ground Structure Based Elliptical Shape Dual Element MIMO Antenna for S-Band Applications", *Progress In Electromagnetics Research C*, Vol. 143, pp. 67-74, 2024.
- [3] M. J. Farhan, "Reconfigurable a Dual-Port Multi-Band Antenna System with High Isolation Tuning Characteristics for Portable Wireless Devices", *International Journal of Intelligent Engineering & Systems*, Vol. 14, No. 5, 2021, doi: 10.22266/ijies2021.1031.38.
- [4] V. N. K. R. Devana and M. R. Avula, "Design and Analysis of Dual Band-Notched UWB Antenna using a Slot in Feed and Asymmetrical Parasitic Stub", *IETE Journal of Research*, Vol. 69, Issue. 1, pp. 284-294, 2023.
- [5] T. Kaiser, F. Zheng, and E. Dimitrov, "An Overview of Ultra-Wide-Band Systems with MIMO", In: *Proc. of the IEEE*, Vol. 97, Issue. 2, pp. 285-312, 2009.
- [6] I. Nadeem and D.-Y. Choi, "Study on Mutual Coupling Reduction Technique for MIMO Antennas", *IEEE Access*, Vol. 7, pp. 563-586, 2018.
- [7] V. N. K. R. Devana and M. R. Avula, "A Novel Dual Band Notched MIMO UWB Antenna", *Progress In Electromagnetics Research Letters*, Vol. 93, pp. 65-71, 2020.
- [8] P. Sehgal and K. Patel, "Dual-Band 4×4 Hexagonal SRR MIMO Antenna with Port Excitation-Controlled Gain and Directivity for WLAN/WiMAX Applications", *Progress In Electromagnetics Research C*, Vol. 135, pp. 55-67, 2023.
- [9] S. K. Gupta, R. Mark, K. Mandal, and S. Das, "Four Element UWB MIMO Antenna with Improved Isolation Using Resistance Loaded Stub for S, C, and X Band Applications", *Progress In Electromagnetics Research C*, Vol. 131, pp. 73-87, 2023.
- [10] T. Upadhyaya, V. Sorathiya, S. Al Shathri, W. E. Shafai, U. Patel, K. V. Pandya, and A. Armghan, "Quad Port MIMO Antenna with High Isolation Characteristics for Sub-6 GHz 5G NR Communication", *Scientific Reports*, Article No. 19088, 2023.
- [11] R. B. Sadineni and D. P. Gowda, "A Novel Densely Packed 4 × 4 MIMO Antenna Design for UWB Wireless Applications", *Sensors*, Vol. 23, No. 21, p. 8888, 2023.
- [12] V. K. Jhunjhunwala, P. Kumar, A. P. Parameswaran, P. R. Mane, O. P. Kumar, T. Ali, S. Pathan, S. Vincent, and P. Kumar, "A Four-Port Flexible UWB MIMO Antenna with Enhanced Isolation for Wearable Applications", *Results in Engineering*, Vol. 24, p. 103147, 2024.
- [13] A. Wu, Y. Tao, P. Zhang, Z. Zhang, and Z. Fang, "A Compact High-Isolation Four-Element MIMO Antenna with Asymptote-Shaped Structure", *Sensors*, Vol. 23, No. 5, pp. 2484, 2023.
- [14] K. Pandya, T. Upadhyaya, U. Patel, V. Sorathiya, A. Pandya, A. J. A. Al-Gburi, and M. M. Ismail, "Performance Analysis of Quad-Port UWB MIMO Antenna System for Sub-6 GHz 5G, WLAN and X Band Communications", *Results in Engineering*, Vol. 22, pp. 102318, 2024.
- [15] J. Nan, H. Zhang, and J. Huang, "Four-Port UWB MIMO Vivaldi Antenna Based on Resistor and Radiant Patch", *Progress In Electromagnetics Research M*, Vol. 118, pp. 11-23, 2023.
- [16] W. Ren, Z.-G. Wang, M. Yang, J. Zhou, and W.-Y. Nie, "Design of a Simple Four-Port UWB-MIMO Antenna Based on Fan-Shaped Isolator", *Progress In Electromagnetics Research M*, Vol. 126, pp. 117-126, 2024.
- [17] A. C. Suresh and T. S. Reddy, "Experimental Investigation of Novel Frock-Shaped Miniaturized 4×4 UWB MIMO Antenna using Characteristic Mode Analysis", *Progress In Electromagnetics Research B*, Vol. 101, pp. 45-61, 2023.
- [18] V. N. K. R. Devana, A. Beno, M. S. Alzaidi, P. B. M. Krishna, G. Divyamrutha, W. A. Awan, P. B. Murali, T. A. H. Alghamdi, and M. Alathbah, "A High Bandwidth Dimension Ratio Compact Super Wide Band-Flower Slotted Microstrip Patch Antenna for Millimeter Wireless Applications", *Heliyon*, Vol. 10, No. 1, pp. e23712, 2024.
- [19] A. J. A. Al-Gburi, "5G MIMO Antenna: Compact Design at 28/38 GHz with Metamaterial and SAR Analysis for Mobile Phones", *Przeglad Elektrotechniczny*, Vol. 2024, No. 4, pp. 171-174, 2024.
- [20] C. A. Balanis, *Antenna Theory: Analysis and Design*, 4th ed., Wiley, 2016.
- [21] A. Kumar, G. Singh, M. K. Abdulhameed, S. R. Hashim, and A. J. A. Al-Gburi, "Development of Fractal 5G MIMO Antenna for Sub 6 GHz Wireless Automotive Applications", *Progress In Electromagnetics Research M*, Vol. 130, pp. 121-128, 2024.
- [22] V. L. N. P. Ponnappalli, S. Karthikeyan, J. L. Narayana, and V. N. K. R. Devana, "A Compact SE-DGS Tapered-Fed Notched UWB Antenna Integrated with Ku/K Band for Breast Cancer

- Detection”, *IETE Journal of Research*, Vol. 70, No. 3, pp. 2298-2308, 2024.
- [23] Z.-G. Wang, W. Ren, W.-Y. Nie, W. Mu, and C. Li, “Design of Three-Band Two-Port MIMO Antenna for 5G and Future 6G Applications Based on Fence-Shaped Decoupling Structure”, *Progress In Electromagnetics Research C*, Vol. 134, pp. 249-261, 2023.
- [24] S. Blanch, J. Romeu, and I. Corbella, "Exact Representation of Antenna System Diversity Performance from Input Parameter Description", *Electronics Letters*, Vol. 39, No. 9, pp. 705-707, 2003.
- [25] A. Ghaloua, J. Zbitou, L. Abdellaoui, M. Latrach, A. Tajmouati, and A. Errkik, "A Novel Configuration of a Miniature Printed Antenna Array Based on Defected Ground Structure", *International Journal of Intelligent Engineering and Systems*, Vol. 12, pp. 211-220, 2018, doi: 10.22266/ijies2019.0228.21.